Determination of electric-field gradients in semiconductors with high precision and high sensitivity

Gert Denninger* and Daniel Reiser

Physikalisches Institut, Universität Stuttgart, Pfaffenwaldring 57, D-70550 Stuttgart, Germany

Wurtzite-type semiconductors such as GaN and ZnO exhibit intrinsic electric-field gradients at the nuclear sites due to the hexagonal lattice symmetry. We have determined these field gradients V_{ZZ} for all the nuclear sites by a magnetic double-resonance scheme. Shallow donors, which are present in these semiconductors either unintentionally or by doping, are used to enhance the nuclear magnetic resonance (NMR) sensitivity through the double-resonance technique. The value V_{ZZ} for ^{67}Zn in ZnO is in excellent agreement with the value obtained by Mössbauer spectroscopy. For the Ga position in GaN and for the O position in ZnO we improved the precision by an order of magnitude compared to previous NMR results. The V_{ZZ} value for the N position in GaN was determined. The field gradients are directly related to the bond ionicities in these III-V and II-VI semiconductors. [S0163-1829(97)01808-0]

I. INTRODUCTION

A direct approach to the measurement of electric-field gradients in crystalline solids is the observation of the electric-quadrupole splittings of nuclear magnetic resonance (NMR) transitions. A prerequisite for such measurements is the presence of nuclei with nonvanishing quadrupole moments Q ($I \geqslant 1$). If the quadrupolar nuclei are sufficiently abundant, possess a convenient gyromagnetic ratio γ, and large single crystals are readily available, this direct NMR approach poses few experimental problems. However, a number of interesting nuclei with quadrupole moments exist in very low natural abundance (e.g., ^{17}O with 3.8×10^{-4} and ^{33}S with 7.5×10^{-3}) or possess rather low γ (e.g., ^{14}N) or both, leading to a reduced NMR sensitivity. In such cases isotopic enrichment and large sample volumes are necessary for NMR investigations, making it difficult if not impossible to investigate thin films, epitaxial layers, quantum wells, interfaces, and surfaces. There is much contemporary interest in NMR investigations of such samples since the crystal structure and the electronic structure can differ from the bulk case.

As an example, consider GaN or ZnO, which crystallize in the hexagonal wurtzite structure with an accompanying electric-field gradient. Thin epitaxial layers of GaN, on the other hand, can be stabilized in the cubic zinc-blende structure[1] with vanishing electric-field gradient. Quantum wells, quantum wires, and other confined structures are expected to exhibit electric-field gradients even in the presence of local cubic site symmetry. In all these cases, traditional NMR methods often lack either the sensitivity or the selectivity for the specific studies of interest.

In this paper we present an alternative approach, which relies on the coupling between nuclear and electronic spins, the hyperfine coupling. The electronic spins can arise from conduction electrons (in metals, organic conductors, or semiconductors) or shallow donors in semiconductors with sufficient overlap of the donor electron wave functions. The electron spin resonance (ESR) must be narrowed either by

motion or by exchange, thereby averaging the hyperfine coupling between the nuclear and the electronic spins and making it possible to measure the Knight and Overhauser shifts, which can both be used as local probes. Since the electronic wave function includes coupling to all the nuclei, interactions like the quadrupolar coupling reflect primarily the field gradient of the unperturbed material. The advantages of measuring the interaction in the double resonance scheme described in the present approach are threefold: (i) an increase in sensitivity due to the detection of the NMR transitions via the ESR, (ii) dynamic nuclear polarization can frequently be used to substantially increase the sensitivity yet further, and (iii) selectivity to the lattice areas of interest is directly afforded by the coupling of the nuclei to the electrons. In the following sections, after a reminder of the basic theory, we describe the experimental setup and present results on the semiconductors GaN and ZnO, which both exhibit electric-field gradients with axial symmetry in the hexagonal wurtzite structure.

II. THEORY

Electronic spins $\underline{S}$ and nuclear spins $\underline{I}$ interact via the hyperfine interaction (hfi) $\underline{I}\,\underline{A}\,\underline{S}$, characterized by the hyperfine tensor $\underline{A}$. This interaction exists in atoms, molecules, and the solid state, for both localized and delocalized electron states. Whereas the hfi is usually resolved in the ESR spectra of radicals in gases and liquids, the inhomogeneous broadening in solids in general results in unresolved hfi structure of the corresponding ESR. In such cases, electron nuclear double resonance (ENDOR) is the method of choice to resolve the hfi,[2] an approach that is only feasible for *isolated* electron centers. As soon as the individual ESR centers interact via an exchange interaction E_{ex}, the correlation time of a particular electronic spin at a particular nuclear position decreases to $\tau_c \cong \hbar/E_{\mathrm{ex}}$. All ENDOR transitions with hfi energies $A \ll \hbar/\tau_c \cong E_{\mathrm{ex}}$ undergo severe broadening, making them unobservable. An extreme case is that of conduction electrons in metals, which are coupled to all the nuclei with a correlation time $\tau_c \cong \hbar/E_F$ for the relevant unpaired elec-

tronic spins at the Fermi energy E_F. With typical values of $E_F \gtrsim 1$ eV, the correlation times in metals are usually of the order of 10^{-15} s or shorter and the hfi between electrons and nuclei is averaged away. Remaining consequences of the hfi are (i) Knight shifts of the NMR lines due to the average electronic polarization $\langle S_z \rangle \neq 0$ and accompanying interaction proportional to $A\langle S_z \rangle$, (ii) Overhauser shifts of the ESR lines due to the average nuclear polarization $\langle I_z \rangle \neq 0$ and accompanying interaction proportional to $A\langle I_z \rangle$, (iii) nuclear spin lattice relaxation via the fluctuating part of the hfi, and (iv) dynamic nuclear polarization effects if the ESR transitions are driven out of thermal equilibrium.

In the case of electron spins interacting via exchange interactions the reasoning is similar to that for conduction electrons. All hfi interactions $A \ll E_{ex}$ are averaged and the corresponding resonance shifts are manifested. A major difference between the cases of conduction and exchange coupled electrons is the temperature dependence of $\langle S_z \rangle$. For conduction electrons the magnetic susceptibility, and thus $\langle S_z \rangle$, is small and essentially independent of temperature (Pauli paramagnetism). Exchange coupled electron systems, on the other hand, behave practically like a Curie spin system with $\langle S_z \rangle \propto 1/T$, as long as the exchange coupling $E_{ex} \ll kT$. This situation is essentially fulfilled for shallow donors in semiconductors in a certain doping range between isolated donors (low N_D) and metallic conduction (high N_D).

A general feature of the band structure of the III-V and II-VI semiconductors is a conduction band with predominantly s-like symmetry and a valence band derived from p-like atomic orbitals. Thus the conduction-band electron-shallow donor wave functions couple to the nuclei via the Fermi-contact-type hyperfine interaction

$$A_{fc} = \frac{8\pi}{3} \frac{\mu_0}{4\pi} (\hbar \gamma_n)(g_e \mu_B)|\psi(\mathbf{r}_k)|^2, \qquad (1)$$

where $|\psi(\mathbf{r}_k)|^2$ is the probability density of the electron at the nuclear position $\mathbf{r}_k$, and $(\hbar \gamma_n)$ and $(g_e \mu_B)$ are the magnetic moments of the nucleus and the electron.

The wave function $\psi(\mathbf{r}_k)$ is usually not known for either the conduction electrons or the shallow donors. In semiconductors with low effective mass m^* of the conduction electrons, the effective-mass theory is an approximation, describing shallow donors as hydrogenlike centers with an effective Coulomb potential $e/(4\pi\varepsilon_0\varepsilon)$. Low effective mass m^* (e.g., 0.2 ± 0.02 for GaN) and high ε (≈ 10 for GaN) yield rather large effective Bohr radii $a_{eff} = a_0\varepsilon/m^*$ ($a_{eff} = 26.5$ Å for GaN) (Ref. 3) and the envelope wave function of the shallow donor ground state is hydrogen s-like:

$$\Phi(r) = \frac{1}{\sqrt{\pi}} \frac{1}{\sqrt{a_{eff}^3}} \exp\left(\frac{-r}{a_{eff}}\right), \qquad (2)$$

where r is the distance from the donor center. As an approximation, the hyperfine coupling of a nucleus of type α at position r_k can be expressed as $A(r_k) = A_\alpha |\Phi(r_k)|^2$, with an ''amplification'' factor A_α, characteristic of the isotope and the substance, but independent of the distance r_k. The theoretical justification for such an approximation[4] and experimental evidence for the validity of this approach[5] have been described previously. The consequence is that all the nuclei

in the range of the shallow donor wave function experience a hfi that falls off exponentially with the distance from the donor center. In contrast to the case of conduction electrons in metals or semiconductors, there is a distribution of coupling constants and the Knight shift and the Overhauser shift can only be calculated by numerical integration over the wave function $\Phi(r)$.

A further consequence of a scalar hfi is that the nuclear polarization can be enhanced considerably by the saturation of the ESR line. This dynamical nuclear polarization (DNP) phenomenon is known as the Overhauser effect.[6] Apart from metals, where it was predicted and observed,[7] DNP is particularly dominant in semiconductors.[8] The consequence of the saturation of the ESR [saturation factor $s = (\langle S_z^0 \rangle - \langle S_z \rangle)/\langle S_z^0 \rangle$, $s = 0$ for no saturation, $s = 1$ for complete saturation] is an enhancement of the nuclear spin polarization $\langle I_z \rangle$ from its thermal equilibrium value $\langle I_z^0 \rangle$:

$$\langle I_z \rangle = \langle I_z^0 \rangle (1 + Vs). \qquad (3)$$

For a scalar hfi of the Fermi contact type the DNP factor V depends only on the ratio of nuclear spin relaxation rate w_e via the electronic spins to the relaxation rate w_0 via other interactions (e.g., quadrupolar relaxation):

$$V = \frac{(g_e \mu_B)}{(g_n \mu_n)} \frac{w_e}{(w_e + w_0)}. \qquad (4)$$

The DNP factor can reach substantial values (e.g., 9106 for ^{14}N and 2735 for ^{69}Ga, both calculated for $g_e = 2$ and no ''leakage'' $w_0 = 0$). It is this large factor V that represents one of the main advantages of double resonance experiments of the Overhauser shift type. The enhanced nuclear polarization $\langle I_z \rangle$ leads to an enhanced Overhauser shift ΔB_{Ov} of the ESR:

$$\Delta B_{Ov} = \Delta B_{Ov}^0 (1 + Vs) = \frac{A_{zz} \langle I_z^0 \rangle}{g_e \mu_B} (1 + Vs), \qquad (5)$$

where ΔB_{Ov}^0 denotes the Overhauser shift at thermal equilibrium and A_{zz} is the tensor component of the hfi in the direction of B. Thus the shift of the ESR by the average polarization of the nuclei can be enhanced by partial saturation of the ESR and can be measured at the same time through the position of the ESR line. Even with the complications of the numerical averaging of the hfi over the shallow donor wave function, the above analysis of the DNP remains basically intact. One has to keep in mind that the DNP is different for nuclei at different distances from the donor center and the factor V has to be interpreted as a suitable numerical average. Detailed numerical analyses for this case are presently under way. Apart from the complication of interpreting the V, DNP can be used to increase the measured ESR signal shifts considerably. Basically one uses the ESR to detect the NMR transitions with high sensitivity and with selectivity to the volume in the range of the donor wave function.

The quadrupole interaction of nuclei with spin $I \geq 1$ affects only the nuclear spins and is not influenced by the motional or exchange averaging. In single crystals with nonvanishing electric-field gradients at the nuclear sites this interaction splits the NMR spectrum into $(2*I - 1)$ lines. The same happens to the Overhauser shift spectrum. In all the

cases discussed in this paper, the electric-field gradient has axial symmetry $V_{ZZ} \neq V_{XX} = V_{YY}$. The indices XX, YY, ZZ refer to the principal axis system of the quadrupole tensor. If as usual the magnetic field is applied along z and the angle $\angle(Z,z)$ is denoted by θ, the quadrupole Hamiltonian is

$$\hat{H} = \frac{e^2 q Q}{4I(2I-1)} \left\{ \tfrac{1}{2}(3\cos^2\theta - 1)[3\hat{I}_z^2 - I(I+1)] \right.$$
$$+ \tfrac{3}{2}\sin\theta\cos\theta[\hat{I}_z(\hat{I}_+ + \hat{I}_-) + (\hat{I}_+ + \hat{I}_-)\hat{I}_z]$$
$$\left. + \tfrac{3}{4}\sin^2\theta(\hat{I}_+^2 + \hat{I}_-^2) \right\}, \tag{6}$$

where Q is the quadrupole moment of the nucleus and $eq = V_{ZZ}$, the electric-field gradient.[9] The Hamiltonian of Eq. (6), together with the Zeeman-Hamiltonian $g_n\mu_n B\hat{I}_z$, can be fully diagonalized (for example, by mathematical programs such as MAPLE or numerically). From a fit of the experimental NMR transitions to the solutions of the Hamiltonian one can determine V_{ZZ} with high precision as shown in the following section.

III. EXPERIMENTAL SETUP

Three major experimental requirements for the successful investigation of hfi interactions by the Overhauser shift technique are the following.

(i) The ESR signal of the conduction electrons/holes or shallow donors/acceptors must be detected with sufficient signal/noise ratio and long-term stability. At least partial saturation of the ESR signal should be possible in order to enhance the nuclear polarization via the DNP effect.

(ii) The NMR of all the relevant nuclei must be nearly completely saturated. Due to the rather low nuclear relaxation rates $1/T_1$ this requires only moderate RF fields B_2.

(iii) Since the measurable Overhauser shifts are often very small ($\Delta B_{Ov}/B_0 \approx 10^{-8}$ or less), high-stability field-frequency locking of the ESR setup is necessary.

These requirements can be accommodated, but not optimally, by using a commercial ENDOR setup. ENDOR resonators are usually designed to provide fairly intense RF fields B_2 and the ESR sensitivity is low compared to standard ESR resonators. We follow a different strategy, placing more emphasis on high ESR sensitivity and only low RF fields. A cavity with a high-quality factor Q and a high filling factor is optimal, since fairly high B_1 fields can saturate the ESR even at low microwave power. The RF field B_2 is produced by a single hairpin loop surrounding the sample and the connection to the RF amplifier is provided by a coaxial cable inside the sample holder. A useful combination used in our X-band work is the dielectric ring resonator (commercially available from Bruker GmbH), which is insensitive to the additional metal from the RF loop. In the Q band (34 GHz) we use the standard low-temperature cylindrical resonator, but the presence of the RF loop considerably lowers the quality factor Q.

Figure 1 shows one of our RF inserts for the dielectric cavity. Solid samples with typical dimensions up to $3\times3\times1$ mm^3 can be directly mounted on a groove in the glass sample rod. Powder samples use a slightly different sample holder. Small angular adjustments can be performed by turning the sample rod, but the RF field B_2 must retain a significant component perpendicular to B_0, thus limiting the angular
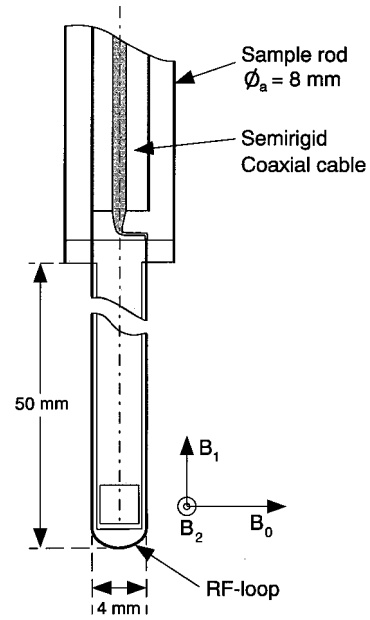

FIG. 1. Sample holder with radio-frequency loop for insertion into the dielectric resonator.

range. Larger angles can be achieved by adjustment of the glass substrate with respect to the loop.

With this setup, the ESR of the shallow donor resonance in the semiconductors GaN and ZnO has been measured and typical results are depicted in Fig. 1 of Ref. 3 and in Fig. 1 of Ref. 23. Both resonances are characterized by a g factor considerably lower than 2: for GaN, $g_\parallel = 1.9503 \pm 0.0001$ and $g_\perp = 1.9483 \pm 0.0001$;[3] for ZnO $g_\parallel = 1.956$ and $g_\perp = 1.955$.[10] Details can be found in Refs. 3 and 11 and the references therein. For the purpose of the present investigation it is only important that both resonances originate from shallow donors[12,11] and the ESR is appreciably exchange narrowed [a factor $\cong 50$ for GaN (Ref. 3)]. This exchange narrowing is essential for the averaging of the hyperfine interaction (see Sec. V) and for the DNP. However, similar results are to be expected for motionally narrowed lines (as in metals). Most ordinary metals, however, have cubic site symmetry and no electric-field gradient. In organic metals the resolved quadrupole splitting of the ^{2}H resonance has been detected in a similar way.[13]

Figure 1 in Ref. 23 shows the somewhat unusual temperature dependence of the ESR linewidth of ZnO, with GaN behaving in a similar manner. The explanation in both cases is the combined action of increasing exchange and increasing scattering by optical phonons and can be correlated to the temperature dependence of the charge carrier mobility.[14] For measurements of the electric-field gradient the temperature range $8\,\text{K} \leq T \leq 50\,\text{K}$ was used, with particularly high sensitivity and precision at $T \cong 10\,\text{K}$. Whereas signal/noise (S/N) considerations would favor lower temperatures, thermal stability of our helium flow cryostat was better at $T = 10-20\,\text{K}$. A further advantage of $T \cong 10\,\text{K}$ is that the nuclear relaxation rates are not too low, permitting fairly rapid repetitive sweeps in the double-resonance experiments.

Double-resonance shift measurements are conducted by locking the B_0 field to resonance through an additional regulated field ΔB_0, realized by a dc offset through the cavity

modulation coils. This scheme offers stability, ease of handling and accurate shift calibration.[15] The dc offset current directly reflects any changes in the resonant field. This signal reflects the resonant Overhauser shift and it is enhanced by repetitive sweeps of the RF through the NMR resonance lines. At higher RF power, the nonresonant Bloch-Siegert shift $\Delta B_{BS} \cong 2(B_2/B_0)^2$ yields a background signal that is irrelevant in these experiments. B_2 is the RF magnetic-field component in the rotating frame. A complete Overhauser shift experiment requires the investigation of the shift as a function of microwave power and RF power at each temperature in order to access both ESR and NMR saturation parameters. In the present case only one set of data near optimum S/N conditions is sufficient to determine the quadrupole splitting and the electric-field gradient V_{ZZ}.

IV. EXPERIMENTAL RESULTS AND DISCUSSION

The GaN sample investigated in this study was a 220-μm-thick free-standing platelet, originally grown on a (0001) oriented sapphire substrate by hydride vapor epitaxy.[16] The concentration of shallow donors was estimated by ESR to be 5×10^{16} cm^{-3} at 5 K. The ESR linewidth is $\Delta B_{pp} \cong 0.5$ mT at 5 K. The ZnO samples were single crystals with a hexagonal habitus, needle shaped with typical dimensions of $1 \times 1 \times 10$ mm^3, and the hexagonal c axis along the needle axis. Sample 1 was nominally undoped, but interstitial Zn leads to a donor concentration of $N_D \cong 5 \times 10^{16}$ cm^{-3}. Samples from the same batch were already characterized by Hall mobility and conductivity measurements in 1974.[17] In addition we investigated a ZnO crystal 2 intentionally doped with Ga, donor concentration $\cong 10^{16}$ cm^{-3}, with a size similar to that of sample 1. With respect to the electric-field gradient measurements no differences were seen within experimental error and results from both samples are presented.

In GaN, as in most III-V semiconductors, nearly all the relevant isotopes possess a nuclear moment (^{69}Ga, $I=3/2$, 60.1% abundance; ^{71}Ga, $I=3/2$, 39.9%, and ^{14}N, $I=1$, 99.63% abundance). Thus the Overhauser shift, proportional to the abundance, is relatively large. An overview shift spectrum is shown in Fig. 2 spanning the range 0.8–18 MHz. All the relevant isotopes result in shift peaks near the free nuclear Larmor frequency and the quadrupole splitting is directly accessible. Due to the rather long nuclear relaxation times (up to a few hundred seconds in GaN at 5 K) the general appearance of an Overhauser shift signal is a steplike decrease near the NMR transition followed by a slow relaxation towards equilibrium. This can be seen very clearly at $\cong 1.1$ MHz for the two transitions of ^{14}N.

In ZnO the isotopes with magnetic moments have low natural abundance (^{67}Zn, $I=5/2$, 4.1% abundance and ^{17}O, $I=5/2$, 3.8×10^{-4} abundance). This is a rather general characteristic of II-VI semiconductors. One consequence is a rather small hyperfine interaction compared to the III-V case, resulting in, e.g., much narrower ESR lines of conduction electrons and shallow donors (5 G in GaN and 0.3 G in ZnO). The resulting Overhauser shift is smaller as well, but due to the narrower ESR line it can be measured with higher precision and high DNP values can easily be achieved. Figure 2 shows an overview result for the $B_0 \perp c$ axis. The expected five transitions of ^{67}Zn are centered near the Larmor
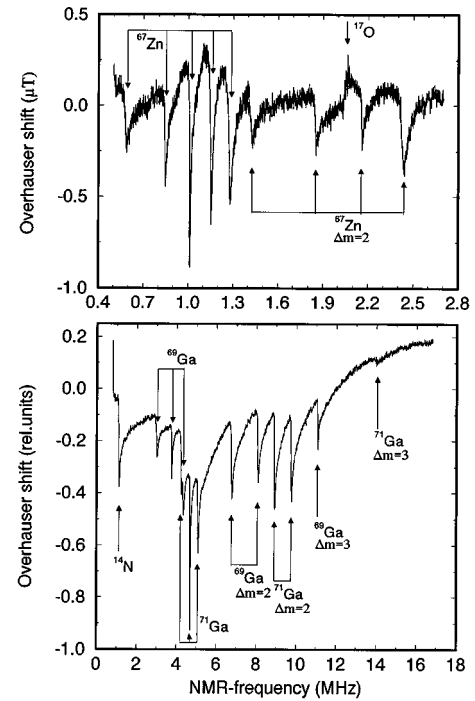

FIG. 2. Overview of the Overhauser shift spectra for GaN and ZnO. Lower part; GaN, $T=8$ K. Upper part: ZnO, $T=8$ K. The origin and the order of the transitions are indicated in the figure.

frequency $\cong 940$ kHz. Since the quadrupole interaction at these low Larmor frequencies (dictated by the ESR frequency of 9.7 GHz) is not small compared to the Larmor interaction, the eigenstates of the effective NMR Hamiltonian are not pure states of $|I, m_I\rangle$. Due to the admixture of all m_I values in all the eigenstates, formal $\Delta m_I = \pm 2, \pm 3, \pm 4$ transitions can be detected. These are clearly visible in Fig. 2 for ^{69}Ga, ^{71}Ga, and ^{67}Zn. In the Ga case with $I=3/2$ we obtain two $\Delta m_I = \pm 2$ transitions and one $\Delta m_I = \pm 3$ transitions for each of the isotopes. In the case of ^{67}Zn with $I=5/2$, the numbers of transitions are 4 for $\Delta m_I = \pm 2$, 3 for $\Delta m_I = \pm 3$, 2 for $\Delta m_I = \pm 4$, and 1 for $\Delta m_I = \pm 5$. Since the shift signals result from saturation of the NMR transitions and do not have to be detected via the transverse magnetization as in NMR spectroscopy, these $\Delta m_I \neq \pm 1$ transitions are intense and easy to measure. This situation applies to GaN as well and here all the transitions $\Delta m_I = \pm 1, \pm 2, \pm 3$ can be seen for both isotopes ^{69}Ga and ^{71}Ga in Fig. 2. No independent information beyond that available from the $\Delta m_I = \pm 1$ can be obtained, but care must be taken not to confuse these transitions with those from other nuclei in the same frequency range. Furthermore, the $\Delta m_I = \pm 2$ transitions, for example, can be driven efficiently by double-quantum transitions, which can be clearly seen in the case of ^{17}O in Fig. 3. All these details must be taken into account when fitting the data to the appropriate model.

More detailed information on the quadrupole splitting was obtained by selectively measuring spectral regions of interest with high resolution. Figure 2 in Ref. 3 shows the results for the two ^{14}N transitions in GaN. A nearly perfect fit to a model including a Lorentzian line shape and a subsequent exponential decay is possible (solid line) and from the fit data we deduce a quadrupole splitting of 20.89 kHz. With
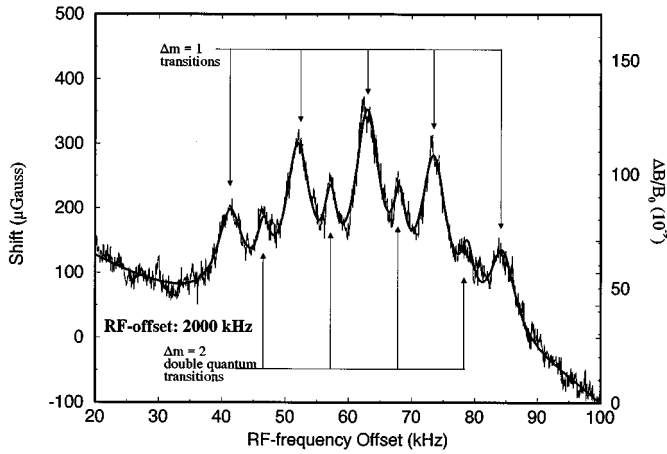
FIG. 3. Overhauser shift of ^{17}O with high resolution. The RF offset is 2000 kHz. The position of the five $\Delta m = 1$ lines is indicated by the dashed vertical lines. The four $\Delta m = 2$, double-quantum transitions are visible between the $\Delta m = 1$ single-quantum transitions. The solid line is a fit to the data including both types of transitions. Note the relative accuracy $\Delta B_{\text{Ov}}/B_0 \approx 10 \times 10^{-9}$.

FIG. 4. Sum of least-squares errors for the five $\Delta m = 1$ transitions of ^{67}Zn versus the angle θ and $e^2 qQ/h$. Three contours of constant error values are shown near the minimum at $\theta_{\min} = 86.74°$ and 2391.88 kHz. The Zeeman plus quadrupole Hamiltonian was diagonalized by MAPLE and fitted to the experimental line positions of all five $\Delta m = 1$ transitions.

the theory of the quadrupolar interaction (see, e.g., the treatment in Ref. 9) and a complete diagonalization of the Hamiltonian, we obtain the electric-field gradient V_{ZZ} at the N position. We quote the quantity $e^2 qQ/h = eQV_{ZZ}/h$ in frequency units and use the known values of the quadrupole moments Q (Ref. 18) to derive the corresponding field gradients V_{ZZ}. Note that the Q values are not always known to the precision of the experiment, so a comparison of the frequencies may be more appropriate.

Taking $eQ = 0.0156 \times 10^{-24}$ cm^2 for ^{14}N, we determine $V_{ZZ} = (0.788 \pm 0.004) \pm 10^{20}$ V m^{-2} at the ^{14}N position. In a similar manner, all the electric-field gradients at the different nuclear positions have been determined. Figure 3 shows the results of a high-resolution measurement of the ^{17}O induced shift. This shift shows the high sensitivity of our double-resonance scheme: the natural abundance of ^{17}O is only 3.8×10^{-4}, resulting in relative shifts $\Delta B_{\text{Ov}}/B_0$ of the order of 10^{-8}. Nevertheless, both the shift itself and the NMR line positions can be determined with high precision due to the stabilization of the spectrometer. In all cases we used a complete diagonalization of the respective spin Hamiltonian for $I = 1$ (^{14}N), $I = 3/2$ (^{69}Ga and ^{71}Ga), or $I = 5/2$ (^{67}Zn and ^{17}O), assuming radial symmetry with respect to the hexagonal c axis ($\eta = 0$). An asymmetry parameter $\eta = 0$ is expected from the crystal symmetry and was confirmed experimentally for the Zn site by Mössbauer spectroscopy.[19] The angle θ and the effective field B_0 were used as fitting parameters together with the quadrupole coupling ν_Q. In all cases the minimum of the sum of least-square differences could be determined unambiguously and with high precision. It even turned out that deviations of the angle θ from 90° due to deviations in mounting could be precisely corrected from the fit of the quadrupole splitting. This is exemplified in Fig. 4, where we show a cut through the fit error versus the angle θ and field gradient $e^2 qQ/h$. The repeatability of the fitting procedure between independent data sets of the same sample is approximately 0.2% and the reproducibility between data sets from different samples is 0.3%. The experimental errors in
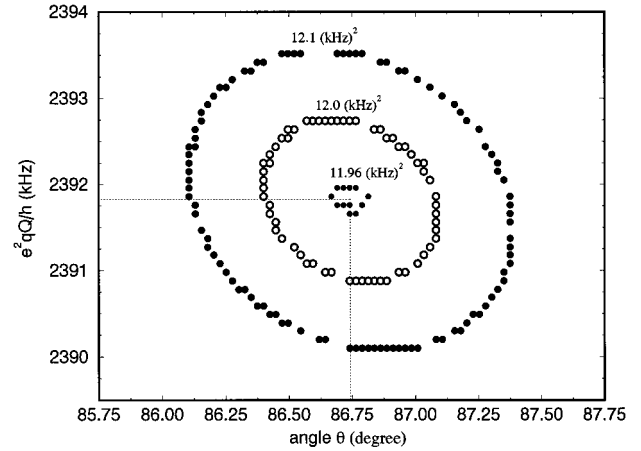
the NMR line positions are difficult to determine directly since these positions are in themselves the result of a nonlinear fit of the data to a model including linewidth and relaxation. Our experimental approach to the overall precision of the field gradient determination was to use results from independent measurements in the case of GaN. Furthermore, in ZnO we compared independent results from different samples with different n-doping concentrations. Individual determinations in ZnO differed by no more than 0.3%; the precision in GaN is slightly worse, 0.5%, limited by a poorer signal/noise ratio of the ESR. Our results are summarized in Table I together with a comparison with existing values from other experiments and from theory. The highest precision reported so far was obtained in a ^{67}Zn Mössbauer experiment on 85.2% ^{67}Zn enriched ZnO powder.[19] The Mössbauer value is 0.37% higher than our ^{67}Zn value and the agreement is within the experimental errors. We are confident, therefore, that our double-resonance scheme yields high-precision measurements of field gradients for the other nuclei as well. Values from NMR powder investigations for the Ga position in GaN (Ref. 20) and for the O position in ^{17}O enriched powders[21] differ by up to 10%, but in these studies no precision is stated. The results of the present work are expected to be of higher precision, considering the indirect NMR approach employed in the linewidth studies of powder samples. Within the limits set by the ESR signal/noise ratio our data also appear to be free of systematic uncertainties.

The purpose of this paper is not to interpret the electric-field gradients but to present reliable, precise results of the field gradients in semiconductors for all the nuclear sites and to stimulate different calculations. The experimental data for ^{67}Zn from Mössbauer spectroscopy[19] have already allowed detailed Hartree-Fock cluster calculations for the Zn site in ZnO.[22] The authors report the result of a $(ZnO_4)^{6-}$ cluster calculation by a Hartree-Fock linear combination of an atomic orbitals–molecular orbital procedure, which yields $V_{ZZ} = 7.1 \times 10^{20}$ V/m^2, only 8% larger than both the Mössbauer value and the value from this work. Similar cluster

TABLE I. Electric-field gradients in GaN and ZnO from this work and comparison to values from other experiments.

Experiment \ Sample isotope	GaN, $T = 8$ K			ZnO, $T = 20$ K	
	^{69}Ga	^{71}Ga	^{14}N	^{67}Zn	^{17}O
eQV_{ZZ}/h (this work)	2.865 ± 0.015 MHz	1.806 ± 0.01 MHz	29.72 ± 0.15 kHz	2.392 ± 0.007 MHz	145 ± 0.45 kHz
Mössbauer spectroscopy (Ref. 19)				2.401 ± 0.004 MHz	
NMR magic angle spinning (Refs. 20 and 21)	2.8 MHz	1.7 MHz			130 kHz
Q (10^{-24} cm^2) (Ref. 18)	0.168	0.106	0.0156	0.150	-0.02578
V_{ZZ} (10^{20} V/m^2)	7.053 ± 0.04	7.046 ± 0.04	0.788 ± 0.004	6.595 ± 0.02	2.326 ± 0.007

calculations should now be possible for the O site and for both nuclear sites in GaN. As an approximation one can calculate the electric-field gradients of the hexagonal crystal structure by using an ionic point-charge model and including the Sternheimer antishielding factors. Details on this approach for GaN and ZnO can be found in Ref. 23. However, due to the unknown covalent contributions of the bond, such an approach is not entirely satisfactory and *ab initio* calculations such as those in Ref. 22 are necessary. Reliable determinations of the bond ionicities in these semiconductors should be possible from the field gradient calculations.

V. CONCLUSION

Electric-field gradients have been determined for all the nuclear sites in two typical semiconductors with wurtzite structure: GaN (III-V) and ZnO (II-VI). The magnetic double-resonance method is of general applicability since the bandstructure of the III-V and II-VI compounds provides an s-type conduction band and shallow donors are present either unintentionally or can be supplied by suitable doping. The high sensitivity of the double-resonance scheme should enable investigations in thin films, interfaces, or even of quantum confined structures, where the electric-field gradients differ from the bulk. An extension of the method to optical detection of magnetic resonance via, e.g., luminescence or circular polarization of the luminescence,[24] should further enable higher sensitivity and selectivity.

ACKNOWLEDGMENTS

[*]Author to whom correspondence should be addressed.

[1]M. Fanciulli, T. Lei, and T. D. Moustakas, Phys. Rev. B **48**, 15 144 (1993).

[2]G. Feher, Phys. Rev. **103**, 834 (1956).

[3]G. Denninger, R. Beerhalter, D. Reiser, K. Maier, J. Schneider, T. Detchprohm, and K. Hiramatsu, Solid State Commun. **99**, 347 (1996).

[4]B. S. Gourary and F. J. Adrian, Phys. Rev. **105**, 1180 (1957).

[5]M. T. Bennebroek, O. G. Poluektov, A. J. Zakrzewski, P. G. Baranov, and J. Schmidt, Phys. Rev. Lett. **74**, 442 (1995).

[6]A. W. Overhauser, Phys. Rev. **89**, 689 (1953); **92**, 411 (1953).

[7]T. R. Carver and C. P. Slichter, Phys. Rev. **102**, 975 (1956).

[8]B. Gotschy, G. Denninger, H. Obloh, W. Wilkening, and J. Schneider, Solid State Commun. **71**, 629 (1989).

[9]A. Abragam, *Principles of Nuclear Magnetism* (Clarendon, Oxford, 1961), Chap. VII, p. 216.

[10]K. A. Müller and J. Schneider, Phys. Lett. **4**, 288 (1963).

[11]W. E. Carlos, J. A. Freitas, Jr., M. Asif Khan, D. T. Olson, and J. N. Kuznia, Phys. Rev. B **48**, 17 878 (1993).

[12]M. Asif Khan, D. T. Olson, J. N. Kuznia, W. E. Carlos, and J. A. Freitas, Jr., J. Appl. Phys. **74**, 5901 (1993).

[13]G. Denninger, Mol. Cryst. Liq. Cryst. **171**, 315 (1989).

[14]K. F. Dombrowski, Diploma thesis, Universität Freiburg, 1995, p. 94.

[15]G. Denninger, Bruker Rep. **1/1987**, 18 (1987).

[16]T. Detchprohm, K. Hiramatsu, K. Itoh, and I. Akasaki, Jpn. J. Appl. Phys. **31**, L1454 (1992).

[17]R. Wagner and R. Helbig, J. Phys. Chem. Solids **35**, 327 (1974).

[18]*Numerical Data and Functional Relationships in Science and Technology*, edited by K. H. Hellwege and A. M. Hellwege, Landolt-Börnstein, New Series, Group III, Vol. 31, pt. a (Springer, Berlin, 1993). and unpublished.

[19]C. Schäfer, W. Potzel, W. Adlassnig, P. Pöttig, E. Ikonen, and G. M. Kalvius, Phys. Rev. B **37**, 7247 (1988).

[20]O. H. Han, H. K. C. Timken, and E. Oldfield, J. Chem. Phys. **89**, 6046 (1988).

[21]G. L. Turner, S. E. Chung, and E. Oldfield, J. Magn. Reson. **64**, 316 (1985).

[22]D. W. Mitchell, S. B. Sulaiman, N. Sahoo, T. P. Das, W. Potzel, and G. M. Kalvius, Phys. Rev. B **44**, 6728 (1991).

[23]D. Reiser, J. Blömker, G. Denninger, and J. Schneider, Solid. State Commun. (to be published).

[24]M. Krapf, G. Denninger, H. Pascher, G. Weimann, and W. Schlapp, Solid State Commun. **74**, 1141 (1990); **78**, 459 (1991).